Elastic approximation for a solar parabolic trough

Gang Xiao

Elastic approximation for a solar parabolic trough

February 29, 2012

Gang Xiao (University of Nice, France)

Abstract

For the production of the reflective surface of a solar parabolic trough concentrator in the form of a parabolic cylinder, a cost effective method is to use the elastic buckling of a flat sheet. However, the surface resulting in such a buckling is only a coarse approximation of the parabola, that is not precise enough for the need of a high quality concentrator.

We propose a method to correct this defect of approximation by applying additional external forces on the buckled sheet. These external forces include an edge torsion force and a pressing force on the sheet. Optimal positions and parameters of these additional forces are computed for various cases, that give a result in theoretical maximal concentration ratio up to 171, so this method offers a very attractive approach for low cost and high efficiency solar energy solutions.

Introduction

A parabolic trough [8] is a concentrating solar thermal energy collector, that uses a mirror in a form of a parabolic cylinder to reflect solar rays towards a receiver tube located at the focus line of the parabola. It has the advantage of being reliable and of low cost, while it can reach a working temperature high enough for efficient power generation.

The geometric precision and manufacturing cost of the parabolic mirror is one of the fundamental factors in the production of a parabolic trough. Traditionally, the support of the mirror is a rigid sheet precisely preformed to the shape of a parabolic cylinder. This constitutes an important part of the cost of the product, because both the rigidity of the material and the precision requirement of the forming process are expensive.

Alternatively, it is possible to make use of the elastic buckling of a flat sheet to form an approximately parabolic cylinder, as under certain conditions, the shape of the buckled flat sheet is usefully close to the parabola [4, 5]. While the cost advantage of this approach is obvious, it only provides a rough approximation that does not meet the precision requirement of a high quality

solar concentrator, nor does it allow any correction of eventual defects of the material or the manufacturing processes.

The aim of the present article is to propose an improved approximation of the parabolic cylinder by the elastic deformation of a flat sheet, by applying additional external forces besides the buckling force. These include a torsion force at each edge of the sheet, and two pressing points in the curve. With optimal amount of the forces and optimal positions of the points, this method leads to an approximation of the parabola with a much higher precision. In practice, the additional forces can be applied using adjustable mechanisms, so that minor defects of the material or the manufacturing can be corrected by adjusting these forces.

We will carry out theoretic calculations on the positions and forces, to deduce the precision of the approximation of the parabola, in terms of the theoretic maximal concentration ratio of the parabolic trough. Some results of the calculations are summarized in Table 1, where optimal values of parameters and theoretical maximal concentration ratios are given for various cases. In practice, the actual correcting forces must be adjusted in the field using optical methods. These optical methods will be explained in a future article.

The final section describes the real products of solar concentrators constructed according to the method. With a highly competitive cost level and a theoretic maximal concentration ratio up to 171, this method offers a very attractive approach for low cost and high efficiency solar energy solutions.

1 The equation of an elastic buckling

The buckling of a flat sheet is simply the development of that of a straight rod on a perpendicular dimension. Therefore it is enough to consider the hinged elastic buckling of a straight uniform rod, whose diameter is supposed to be infinitesimally small. When the two edges of the rod is compressed to some extent, the rod will elastically deform to a curved shape; it is this shape that we want to determine. The principle is classical[1], but in most literature the equations are deduced assuming that the deformation of the rod is small, which is not our case. So we re-deduce the equation here using the curvature instead of the second derivative to take into account the fact that the resulting curve is far from straight. The discussion also serves to set up the framework for later development.

Suppose that the original rod is under a horizontal position, and that its weight is infinitesimal, so that there is no effect of the gravity. In this case, the buckled rod forms a curve as in Figure 1.

We will make use of the following notations.

$y = y(x)$	The mathematical function of the curve.
(x, y)	The coordinates of a point on the curve.
(x_0, y_0)	The starting edge of the curve.

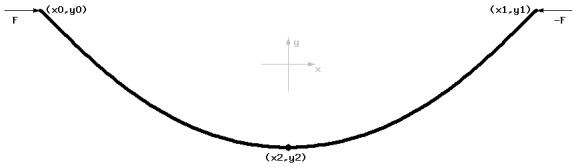

Figure 1: The buckling curve

(x_1, y_1)	The ending edge of the curve.
(x_2, y_2)	The bottom of the curve, that is, where the tangent is horizontal.
W	The opening width of the curve: $W = x_1 - x_0$.
Δ	The maximal depth of the curve: $\Delta = y_0 - y_2$.
Λ	The arc length of the curve, from (x_0, y_0) to (x_1, y_1).
$y'(x)$	The derivative is the slope of the curve at (x, y).
y'_0	$= y'(x_0)$.
θ_0	The tangent angle of the curve at the starting edge: $\theta_0 = \arctan(y'_0)$.
θ_1	The tangent angle of the curve at the ending edge: $\theta_1 = \arctan(y'_1)$.
$\kappa(x)$	The curvature of the curve at (x, y). We have $$\kappa(x) = \frac{y''(x)}{\left(1 + y'(x)^2\right)^{3/2}} .$$.
$\lambda(x)$	The arc length of the curve from (x_0, y_0) to (x, y).
(x_2, v_r)	The position of the solar receiver.
r	The elastic coefficient of the material.
F	The external force at the starting edge. Its direction is horizontal.

The fundamental fact on elasticity is that the curvature of the curve at a point (x, y) is proportional to the moment of force exercised on that point [2, p. 218], once the thickness is infinitesimal. As this moment is equal to $F(y - y_0)$, we have the following equation.

$$\kappa(x) = -\frac{F}{r}(y - y_0) \tag{1}$$

Substituting the formula of $\kappa(x)$, we get the differential equation for the buckled curve:

$$y'' = -\frac{F}{r}(y - y_0)\left(1 + y'^2\right)^{3/2} \tag{2}$$

Under the hypotheses, the curve is symmetric, that is, $y_1 = y_0$ and $\theta_1 = -\theta_0$. By symmetry, the computation needs only be done on the first half of the curve, for the interval $[x_0, x_2]$. And we can fix the first boundary conditions $x_0 = y_0 = 0$, so that the curve is determined by the second boundary condition on y'_0, or in other terms, the starting angle θ_0.

Moreover, it is clear from (1) that the coefficient $\frac{F}{r}$ only affects the scaling of the curve, that is, curves obtained from the equation (2) with different values of $\frac{F}{r}$ are all similar. So we can simplify the situation by putting $\frac{F}{r} = 1$. As a result, the equation becomes

$$y'' = -y\left(1 + y'^2\right)^{3/2} \ . \tag{3}$$

Note that the ending point (x_2, y_2) will be derived from the equation and from the condition $y'_2 = 0$.

Now it is easy to solve (3) by the numerical method that incrementally compute x, y, y', y'' step by step, starting from (x_0, y_0). Here is the PARI/GP code for doing so [9].

```
\\ source code for PARI/GP
\\ Computation of the buckling curve, uncorrected.

\p 10
step=0.00001;    \\ numeric tep
x0=0;            \\ x0
y0=0;            \\ y0
y10=-1;          \\ starting derivative
y20=0;           \\ second derivative
yf=-0.08033;             \\ position of the receiver
sunrad=0.005;            \\ Sun's angular radius
arc=0;
prints=10;       \\ number of points to print; approximative
counter=0;       \\ step counter

printstep=floor(1/prints/step);
one_step()={
 x+=step;
 y=y+y1*step;
 y2=-y*(1+y1^2)^(3/2);
 y1+=y2*step;
 arc+=step*sqrt(1+y1^2);
 counter ++;
```

```
}

dist()={         \\ Computes upper and lower bounds of the cone
        \\ image distance from the center of the receiver
D=sqrt((x-xend)^2+(y-yf)^2);
 ss=1+y1^2;      \\ vector length;
        \\ the vector of reflected light is
        \\ (2y',(y'2-1))
 d0=((x-xend)*(y1^2-1)-2*(y-yf)*y1)/ss; \\ scalar product
 d1=d0+D*sunrad;         \\ upper bound
 d2=d0-D*sunrad;         \\ lower bound
 if(d1>maxup,maxup=d1);
 if(-d2>maxdn,maxdn=-d2);
}

output()={
 print(x" "y" "y1" "y2" "d1" "d2);
}

\\ First pass
x=x0;y=y0;y1=y10;y2=y20;arc=0;
while(y1<=0,one_step())
xend=x;
yend=y;
W=2*xend;

\\ Second pass
maxup=0; maxdn=0;
x=x0;y=y0;y1=y10;y2=y20;arc=0;
dist();
output();        \\ The starting point
while(y1<=0,one_step();dist();if(counter%printstep==0,output()))
output();        \\ The ending point
conc=xend/max(maxup,maxdn);     \\ maximal concentration ratio

print("arc length = "arc);
```

The above code gives the following series of points on the curve for $y_0' = 1$, where each point is given with 4 coordinates (x, y, y', y'').

```
0 0 -1 0
0.1000000000 -0.09953221936 -0.9860368501 -0.2756859273
0.2000000000 -0.1963408827 -0.9461824924 -0.5122921682
0.3000000000 -0.2880793762 -0.8856742047 -0.6866916915
0.4000000000 -0.3730056510 -0.8110227678 -0.7961633051
0.5000000000 -0.4500152186 -0.7282353777 -0.8519394795
0.6000000000 -0.5185367010 -0.6418879099 -0.8700535166
0.7000000000 -0.5783766011 -0.5549848958 -0.8652292941
0.8000000000 -0.6295739172 -0.4692325979 -0.8485675532
0.9000000000 -0.6722890909 -0.3854144589 -0.8275253588
1.000000000 -0.7067287159 -0.3037169806 -0.8067429240
```

```
1.100000000  -0.7330983739  -0.2239652059  -0.7889471528
1.200000000  -0.7515747727  -0.1457765891  -0.7756615439
1.300000000  -0.7622901128  -0.06865549773  -0.7676873373
1.389620000  -0.7653650869 0.000005962117050  -0.7653650869
arc length = 1.633582129
```

Instead of the curve itself, the defects of the buckling curve as an approximation of the parabola are more easily shown by the comparison of the curvatures of the two curves, or equivalently, the comparison of the second derivatives. Note that y'' is constant for the parabola. The second derivatives of the buckling curve, as computed by the numerical algorithm, is shown in Figure 2.

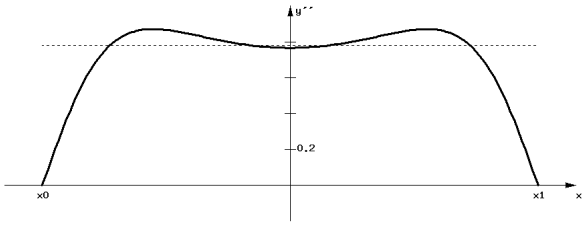

Figure 2: y'' for the buckling curve, $y'_0 = -1$.

With respect to the constant y'' for the parabola, Figure 2 shows two main approximation errors of the buckling curve: the most important is the insufficient curvature near the edges; in fact, the curvature reaches zero towards the edges. The second defect is that in the middle of the curve, there are two small shoulders where the curvature is slightly too high. These shoulders severely limit the usable concentration ratio even if one sacrifices the reflections near the edges of the mirror.

2 Optical interpretation

When a surface is used for reflecting solar radiations, the tangent direction of the surface at each point is more important than the position of the point. Therefore, the effect of the imperfect approximation to the parabola by the elastic buckling of a flat sheet must be studied via ray tracing. This is done in the following manner.

Let C be a symmetric curve as in Figure 3, given by the function $y = y(x)$, that surves as a mirror to reflect solar radiations. The solar radiation beam R_1 comes vertically down to meet the curve C at a point (x, y), and the reflected radiation R_2 is the reflection symmetry of R_1 with respect to the normal line N of the curve at (x, y).

Let (x_f, y_f) be the center of the receiver. We assume $x_f = x_2$ as what is normally the case. Then the optical precision of the curve C can be described by the minimal distance $d(x)$ between the line R_2 and the point (x_f, y_f).

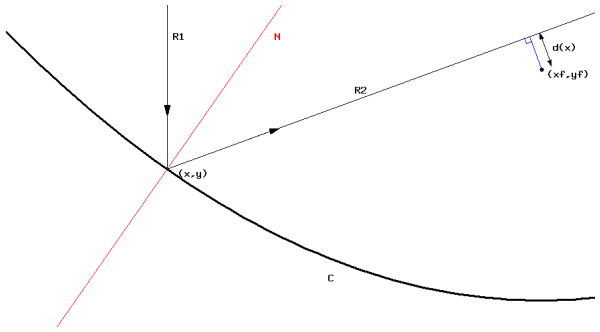

Figure 3: Ray tracing on the reflective curve

Now let (x_r, y_r) be the point of reflection as in Figure 3. The equation of R_1 is $X = x_r$, that of the normal line N is $(X - x_r) + y'(x_r)(Y - y(x_r)) = 0$, therefore the reflected beam R_2 has the equation [12]

$$2y'(x_r)(Y - y_r) = \left(y'(x_r)^2 - 1\right)(X - x_r) \ , \tag{4}$$

and its distance to the point (x_f, y_f) is given by the formula

$$d(x_r) = \frac{\left(y'(x_r)^2 - 1\right)(x_f - x_r) - 2y'(x_r)(y_f - y_r)}{y'(x_r)^2 + 1} \ . \tag{5}$$

Note that we define $d(x_r)$ as a signed value.

If C is a perfect parabola and (x_f, y_f) is the focus of the parabola, it is easily seen from (5) that $d(x) = 0$ for all points (x, y) on C.

The precision of a reflective surface must be measured by the maximal concentration ratio it offers. When C is not the parabola, there is no obvious position for the "focus" y_f, and the concentration ratio depends on the value of y_f. Moreover, in order to compute this maximal concentration ratio, the Sun's angular diameter must be taken into account. Theoretically, this angular diameter varies from 9.2 mrad to 9.5 mrad [7], but due to the atmospheric scattering, the effective angular diameter for a solar concentrator is always slightly larger. So we will take the value of 10 mrad in our computations.

The solar radiations hitting a point on the reflective mirror is not a single beam line, but a cone of beams of angular diameter 10 mrad. As a result, the reflected radiations also form a cone of the same angular diameter. When the latter cone reaches the receiver located at distance D from the reflecting point, the cone's image is a disk of diameter $D/100$. In particular, the receiver's diameter should not be smaller than $D/100$, or part of the reflected radiations would be lost.

Assuming that the receiver of the concentrator is in perfect circular form, let us define the concentration ratio to be the ratio of the opening width W of the reflective mirror to the diameter of the receiver. Under this definition, the

theoretical upper limit of the concentration ratio for a one-dimensional concentrator is 200, because the maximal value of D is at least $W/2$. This upper limit can be reached when C is a perfect parabola with $y'(x_0) = -1$.

The situation is more complicated for the buckling curve, so we can only show some examples with given positions of y_f. For each reflecting point (x, y) on C, we can approximately take

$$d_1(x) = d(x) + \frac{D(x)}{200}\ ,\ d_2(x) = d(x) - \frac{D(x)}{200}$$

as reslectively the upper and lower bounds of the reflected cone, as distances to the center of the receiver. We approximately take $D(x) = \sqrt{(x - x_f)^2 + (y - y_f)^2}$.

For $y'(x_0) = -1$ and $y_f = 0.08033$, Figure 4 shows the lower and upper bounds of the reflected cone, in terms of the minimal distance of the cone's boundary to the center of the receiver, for all the reflecting points (x, y). This is the best position for the maximal concentration ratio if all the reflected radiations are to be intercepted. But one can read from Figure 4 that the maximal concentration ratio will not exceed 16, which is not of any serious use in practice.

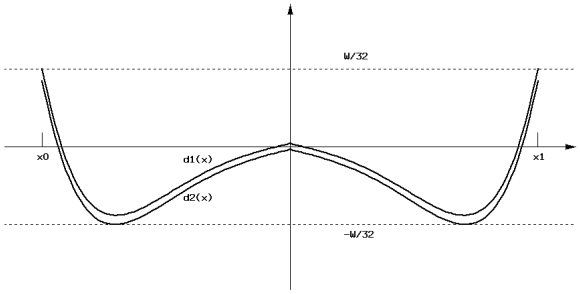

Figure 4: Cone positions for $v_r = -0.08033$

Figure 5 shows the same bounds for $y'(x_0) = -1$ and $y_f = -0.15$. This position of the receiver is optimized in case that radiations reflected from zones near the edges are sacrificed. Note that in this case, the maximal concentration ratio is rather close to 63 but not 73, because the fact of throwing away edge-reflected radiations reduces the effective opening width of the solar concentrator. Adding other inevitable errors, the usable concentration ratio would be below 50.

3 Correcting the buckling curve

Our aim is to correct the two defects of the y'' curve (Figure 2) of the buckling curve: the gradual drop of the curvature towards zero near the edges, and the two shoulders of the curvature in the middle.

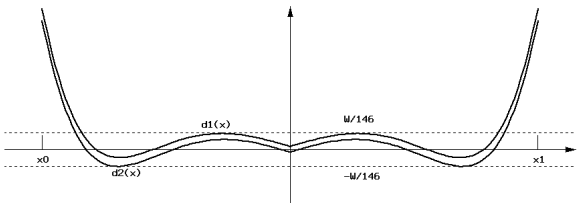

Figure 5: Cone positions for $v_r = -0.15$

Select two symmetric points (x_p, y_p) and (x_q, y_q) on the curve, as shown in Figure 6. As the position of the curve cannot be determined before the computation, these points will be defined by the arc length λ_p from (x_0, y_0) to (x_p, y_p). By symmetry, λ_p is also equal to the arc length from (x_q, y_q) to (x_1, y_1).

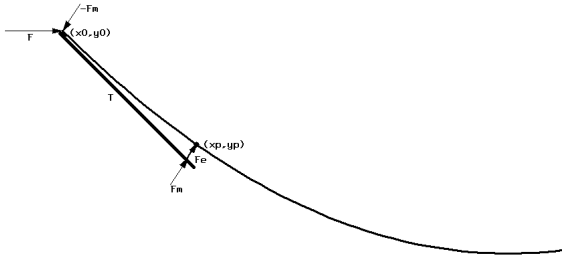

Figure 6: Correction forces applied on the buckling curve

The first correction force applied to the rod is an edge torsion applied through a supposedly rigid mechanism T with one end sealed to the edge of the rod and another end exercising a pressure on the point (x_p, y_p). Let the pressing force of the second end be F_e, and let $k_e = F_e/r$. In this setting, the torsion force has no effect on points (x, y) such that $x > x_p$. For $x \leq x_p$, the effect on the curvature $\kappa(x)$ is equal to

$$k_e \sqrt{(x - x_p)^2 + (y - y_p)^2} \cos(\alpha) \ ,$$

where α is the angle between the vector $(x - x_p, y - y_p)$ and the tangent vector of C at (x_p, y_p). As the curvature of C near the edge is very small, it is safe to make an approximation by replacing $\sqrt{(x - x_p)^2 + (y - y_p)^2}$ by the arc length $\lambda_p - \lambda(x)$ and $\cos(\alpha)$ by 1. So we get the following equation on the effect of the torsion on the curvature of the curve.

$$\kappa_e(x) = \begin{cases} k_e(\lambda_p - \lambda(x)) & \text{if } x \le x_p \\ 0 & \text{if } x > x_p \end{cases} \tag{6}$$

The position of the pressing point (x_p, y_p) is very important. A simple-minded twisting of the edges without pressing point, as proposed in [3], does not give a satisfactory correction of the curve, because while correcting the drop of curvature near the edges, such a mechanism will worsen the "shoulder effect" seen in Figure 2.

Secondly, we add a *pressing force* F_m on the point (x_p, y_p) (and symmetrically on (x_q, y_q) too), to the normal direction of the curve. As a vector, we can write its decomposition into coordinate components

$$F_m = (\sin(\theta_p) F_m, \cos(\theta_p) F_m) \ ,$$

where $\theta_p = \arctan(y'(x_p))$ is the tangent angle of C at (x_p, y_p). Let F_{mh} and F_{mv} be the amplitudes of the two components:

$$F_{mh} = -\sin(\theta_p) F_m = \frac{-y'(x_p)}{\sqrt{1 + y'(x_p)^2}} F_m \ ,$$

$$F_{mv} = \cos(\theta_p) F_m = \frac{F_m}{\sqrt{1 + y'(x_p)^2}} \ .$$

Here we have a minor problem that $y'(x_p)$, hence θ_p, cannot be determined in advance. Fortunately, in practice F_m is small with respect to F, so that one can take an initial value of θ_p then make successive runs of the numerical algorithm, each time replacing θ_p by the value computed from the preceding run. The series of the successive values of θ_p converges very fast.

Let $k_m = F_m/r$, $k_{mh} = F_{mh}/r = -\sin(\theta_p) k_m$, $k_{mv} = F_{mv}/r = \cos(\theta_p) k_m$. For the directions shown in Figure 6, the effect of the pressing force on the curvature of C is as follows.

$$\kappa_m(x) = \begin{cases} 0 & \text{if } x \le x_p \\ k_{mv}(x - x_p) - k_{mh}(y - y_p) & \text{if } x > x_p \end{cases} \tag{7}$$

Note that F_m is an external force that must draw its reactive force at the edge of the curve. In other words, the total external force applied to (x_0, y_0) is now the vector $(F - F_{mh}, -F_{mv})$. Its effect on the curvature should be modified to

$$\kappa_1(x) = (k_{mh} - 1)(y - y_0) - k_{mv}(x - x_0) \ . \tag{8}$$

Now the total effect of the 3 forces on the curvature is $\kappa(x) = \kappa_1(x) + \kappa_e(x) + \kappa_m(x)$. Combining (6), (7), (8) and with normalizing conditions $F/r = 1$ and $x_0 = y_0 = 0$, we get the differential equation for the corrected buckling curve:

$$\kappa(x) = \begin{cases} -k_{mv}x + (k_{mh} - 1)y + k_e(\lambda_p - \lambda(x)) & \text{if } x \le x_p \\ -k_{mv}x_p + k_{mh}y_p - y & \text{if } x > x_p \end{cases} \ . \tag{9}$$

This equation can be numerically solved using the same algorithm as in Section 1, with the subroutine `one_step()` replaced by the following code.

```
one_step_corrected()={
 x+=step;
 y=y+y1*step;
 if(arc<=lambda_p, xp=x;yp=y;y1p=y1);
 kappa1=-kmv*x+(kmh-1)*y+ke*(lambda_p-arc);
 kappa2=-kmv*xp+kmh*yp-y;
 if(arc<=lambda_p, kappa=kappa1, kappa=kappa2);
 y2=y2*sqrt(1+y1^2)^(3/2);
 y1+=y2*step;
 arc+=step*sqrt(1+y1^2);
 counter ++;
}
```

The main parameters of the correction setup are summarized in the following list.

λ_p The arc length that defines the points to exercise correcting forces.

k_e The uniformized edge torsion force.

k_m The uniformized pressing force.

θ_p The tangent angle of C at (x_p, y_p).

y_f The position of the receiver.

Now for a given set of initial values and parameters $\{y_0', \lambda_p, k_e, k_m, y_f\}$, the numerical method similar to that in Section 1 can be applied to solve (9) and compute the value of maximal concentration ratio. Then standard optimization methods such as multiple line search can be applied to optimize the parameter set $\{\lambda_p, k_e, k_m, y_f\}$ and get the optimized maximal concentration ratio ρ for a given initial value y_0'. Table 1 gives the results of the optimization for selected values of y_0'. We are putting $k_m = 0$ in some lines of the table, because the values of ρ thus obtained are already useful, so that the mechanism for adding the pressing force may be removed for these cases.

y_0'	θ_0	λ_p/Λ	$y'(x_p)$	k_e	k_m	y_f	W	ρ
-0.95	43.5°	0.2095	−0.5942	0.36	0	0.0708	2.812	168
-1	45°	0.19	−0.6659	0.4	0	0.0012	2.797	157
-1	45°	0.2	−0.6473	0.36	0.03	−0.001	2.84	171
-1.05	46.4°	0.185	−0.7182	0.3627	0	−0.0705	2.7764	110
-1.05	46.4°	0.2075	−0.6684	0.3039	0.1095	−0.0734	2.949	166
-1.1	47.7°	0.208	−0.7024	0.279	0.17	−0.1445	3.03	153

Table 1: The optimized maximal concentration ratios

We remark that the great concentration ratios up to 171 in Table 1 are neither reachable nor desirable in practice. They are not reachable because other errors will add to the imperfection, such as deformations, manufacturing errors, surface irregularities, etc. And they are not desirable because the high concentration ratio implies a very thin receiver tube, too thin to be practically useful. In practice, a concentration ratio around 100 would be more or less the upper limit. However, the much higher theoretical maximal concentration ratio is necessary to guarantee that this practical concentration ratio can be obtained at reasonable production costs.

Figures 7 and 8 give respectively the y'' curve and the bounds of the reflected cone on the receiver for the case of $y'_0 = -1$, $\rho = 171$.

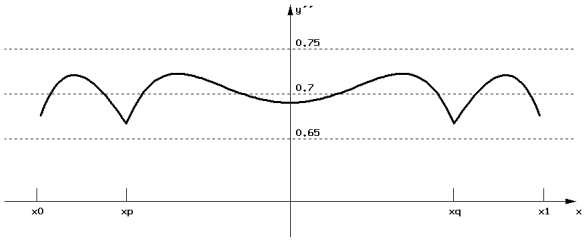

Figure 7: y'' curve of the corrected buckling curve for $y'_0 = -1$.

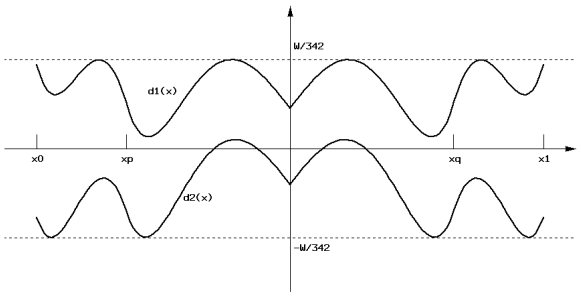

Figure 8: Bounds of the reflected cone for the corrected curve with $y'_0 = -1$.

4 Effective realizations

Various flat sheet materials can be used to construct the reflective sheet: plastics, aluminium, steel. For each of these materials, there is an upper limit of the thickness that must be respected, in order that the deformation of the sheet does not create stress in the material that exceeds its yield strength. Table 2

gives the limit of the thickness for some common materials, assuming a usable strength at 60% of the yield strength and $y_0' = -1$.

Material	stainless steel	iron	alu. alloy	PS
Young's modulus	$200GPa$	$200GPa$	$70GPa$	$3GPa$
Yield strength	$300MPa$	$200MPa$	$240MPa$	$50MPa$
Usable strength	$180MPa$	$120MPa$	$140MPa$	$30MPa$
Max. thickness	$W/1100$	$W/1670$	$W/500$	$W/100$

Table 2: Maximal thickness of materials

The actual concentration ratio of the collector is determined by the diameter of the receiver tube, so it can be changed simply by replacing the receiver.

Several models of concentrating solar collectors have been constructed since 2008, using the corrected elastic reflective surface and according to the closed collector design principle described in [11].

Figure 9 shows an experimental collector model made in plastics sheets. The collector has a width of $0.86m$ and a length of $1m$. The reflective back is a mirror-plated PS sheet with a thickness of $2mm$. The original sheet is not perfectly flat, but the slight irregularities have been compensated by the correction mechanisms without much difficulty.

Figure 9: A plastic collector model

The front picture at the left shows the collector under tracking with a receiver tube of diameter $10mm$. Hence the concentration ratio is 86 times, with a very satisfactory intercept factor. The only noticeable areas where the reflected radiations miss the receiver is near the joining pieces between the back and the end sheets, as the joining pieces and their fixating bolts create local stress and local deformation in the reflective sheets. One can see this phenomenon from the image of the receiver in the front picture of the collector: This image is perfectly straight except at the joining region of the back and the end.

The edge correction mechanism is composed of regularly spaced metal rods, one end of them being fixed on a solid bar running along the edge of the reflective back sheet. The solid bar evenly distributes the torsion force exercised by the rods to the whole edge of the back sheet.

The pressing force is exercised by two steel wires pressing on two aluminium angles running along the back. For experimental reasons, the two aluminium angles are not placed at the computed optimal positions in the picture.

Water is circulating in the receiver to prevent it from overheating.

Figure 10 gives a detailed view of the edge correction mechanism on the back of an improved solar collector model. There is a glidable wire cursor on each rod, whose position determines the strength of the edge correction force.

Figure 10: Edge correction mechanism

References

[1] Timoshenko & Gere, Theory of elastic stability, McGraw-Hill 1961

[2] Ferdinand P. Beer, E. Russell Johnston, Jr., John T. DeWolf, Mechanics of materials 3rd edition, Mc Graw Hill 1972

[3] R. Dame, Adjustable solar concentrator, US patent 4106484, 1978

[4] D. Landridge et al., Solar radiation reflector, PCT patent application WO 80/02604, 1980

[5] P.G. McCormick, Optical evaluation of cylindrical elastical concentrators, Solar Energy Volume 26, Issue 6, 1981, Pages 519-523

[6] R. C. Reuter Jr. & R. K. Wilson, Deformation of a Thin, Elastic Plate to a Deep Parabolic Cylinder, J. Appl. Mech. Volume 50, Issue 1, 221, 1983

[7] W.B.Stine & R.W.Harrigan, Solar Energy Systems Design, John Wiley 1985. Updated version available online from http://www.powerfromthesun.net/

[8] H. Price et al., Advances in parabolic trough solar power technology, J. Sol. Energy Eng. Volume 124, Issue 2, 2002

[9] C. Batut, K. Belabas, D. Bernardi, H. Cohen, M. Olivier, User's guide to PARI/GP, 2000-2003. Available online from http://pari.math.u-bordeaux.fr/

[10] Yu. P. Rylov, Elastically deformed thin-walled solar energy concentrators, Technical Physics Volume 48, Number 11, 2003, 1480-1485, DOI: 10.1134/1.1626784

[11] G. Xiao, A closed parabolic trough solar collector, HAL-00177601, 2007

[12] Reflection (mathematics) in Wikipedia, http://en.wikipedia.org/wiki/Reflection_%28mathematics%29